Survival of cancer stem-like cells under metabolic stress *via* CaMK2α-mediated upregulation of sarco/endoplasmic reticulum calcium ATPase expression

Ki Cheong Park[1,2], Seung Won Kim[1,3], Jeong Yong Jeon[1,4], A Ra Jo[1,2], Hye Ji Choi[1,2], Jungmin Kim[1,2], Hyun Gyu Lee[5], Yonjung Kim[6], Gordon B. Mills[7], Sung Hoon Noh[2], Min Goo Lee[3], Eun Sung Park[8], and Jae-Ho Cheong[1,2,8,9*]

[1]Brain Korea 21 PLUS Project for Medical Science, Yonsei University College of Medicine, Seoul 120-752, South Korea

[2]Department of Surgery, [3]Severance Biomedical Science Institute, [4]Nuclear Medicine, [5]Microbiology and Immunology, [6]Pharmacology, Yonsei University College of Medicine, Seoul 120-752, South Korea

[7]Department of Systems Biology, the University of Texas MD Anderson Cancer Center, Houston, TX, USA

[8]Open NBI Convergence Technology Research Laboratory, [9]Department of Biochemistry & Molecular Biology, Yonsei University College of Medicine, Seoul 120-752, South Korea.

Running title: CSC survival *via* up-regulation of SERCA by CaMK2α

Financial support: Jae-Ho Cheong: National Research Foundation of Korea (NRF) grant funded by the Korean government (MSIP) (No. NRF-2011-0030086) and Korea Health Technology R&D Project through the Korea Health Industry Development Institute (KHIDI), funded by the Ministry of Health & Welfare (No. HI14C1324). Faculty Research Grant funded by Yonsei University College of Medicine (6-2010-0153). Min Goo Lee: grant no. 2013R1A3A2042197 from the NRF.

Conflict of Interest: None declared

[*]**Correspondence:**

Jae-Ho Cheong M.D., Ph.D.

Professor

Department of Surgery,

Yonsei University College of Medicine

50-1, Yonsei-ro, Seodaemun-gu, Seoul 120-752, South Korea

Tel: +82-2-2228-2094

Fax: +82-2-313-8289

E-mail: JHCHEONG@yuhs.ac.

Manuscript information: Word count (excluding Abstract, References, and Figure legends): 4425; 6 main figures, 1 supplementary table.

Statement of Translational Relevance

CaMK2 has been shown to be upregulated in drug-resistant subpopulations of tumor cells and oncogene ablation-resistant cancer stem like cells. The present study demonstrated that CaMK2 plays a critical role in the induction of anti-apoptosis factors *via* NFκB in metabolic stress-resistant tumor cells, which share the characteristics of cancer stem-like cells. In cancer stem-like cells, NFκB transcriptionally induces sarco/endoplasmic reticulum Ca2+-ATPase (SERCA), major calcium transporters, thereby restoring the overloaded cytosolic Ca^{2+}, thus evading potential injury and apoptosis. A combination therapy comprising 2-deoxy-D-glucose and a SERCA inhibitor (thapsigargin) effectively suppressed tumor growth in mouse tumor models, confirming the target selective effect of this strategy. The results implied that CaMK2-mediated induction of SERCA is a central mechanism of metabolic stress-resistant cell survival. Clinically, these observations have significant implications for the development of novel combinatorial strategies that selectively target the vulnerabilities of highly malignant cells such as drug-resistant and cancer stem like cells.

ABSTRACT

Purpose: Cancer cells grow in an unfavorable metabolic milieu in the tumor microenvironment and are constantly exposed to metabolic stress such as chronic nutrient depletion. Cancer stem-like cells (CSCs) are intrinsically resistant to metabolic stress, thereby surviving nutrient insufficiency and driving more malignant tumor progression. In this study, we aimed to demonstrate the potential mechanisms by which CSCs avoid Ca^{2+}-dependent apoptosis during glucose deprivation.

Experimental design: We investigated cell viability and apoptosis under glucose deprivation, performed genome-wide transcriptional profiling of paired CSCs and parental cells, studied the effect of calcium/calmodulin-dependent protein kinase 2 alpha (CaMK2α) gene knockdown, and investigated the role of nuclear factor kappa B (NFκB) in CSCs during time-dependent Ca^{2+}-mediated and glucose deprivation-induced apoptosis. We also observed the effect of combined treatment with 2-deoxy-D-glucose, a metabolic inhibitor that mimics glucose deprivation conditions in mouse xenograft models, and thapsigargin, a specific inhibitor of sarco/endoplasmic reticulum Ca^{2+}-ATPase (SERCA).

Results: We demonstrated the coordinated up-regulation of SERCA in CSCs. SERCA, in turn, is transcriptionally regulated by CaMK2α *via* NFκB activation. Combined treatment with 2-deoxy-D-glucose and thapsigargin, a specific inhibitor of SERCA, significantly reduced tumor growth compared to that in untreated control animals or those treated with the metabolic inhibitor alone.

Conclusions: The current study provides compelling evidence that CaMK2α acts as a key anti-apoptosis regulator in metabolic stress-resistant CSCs by activating NFκB. The latter induces expression of SERCA, allowing survival in glucose-deprived conditions. Importantly, our combination therapeutic strategy provides a novel approach for the clinical application of

CSC treatment.

INTRODUCTION

Metabolic stress, elicited by deprivation of key nutrients such as glucose, is a critical condition that significantly affects cell viability if prolonged. However, cancer stem-like cells (CSCs) have developed molecular strategies to cope with a lack of nutrients, including metabolic and transcriptional reprogramming, to protect cellular bioenergetics [1-3]. The acquisition of survival mechanisms in extreme nutrient-deficient conditions is an important characteristic of CSCs that distinguishes them from non-stem-like cancer cells [4, 5]. Previously, we demonstrated that chronic metabolic stress induced the emergence of CSCs through reprogrammed Wnt signaling [5]. Notably, these CSCs exhibited resistance to glucose deprivation-induced apoptosis by altering NAD^+ metabolism, which is mechanistically related to Ca^{2+} signaling [6].

Glucose deprivation causes endoplasmic reticulum (ER) stress by interfering with N-linked protein glycosylation. ER stress is an important adaptive cellular process that is induced by a range of stimuli and pathological conditions, and triggers evolutionarily conserved molecular responses [7]. The importance of Ca^{2+} signaling in cell death and survival has been studied in response to ER stress [8, 9]. ER stress can cause Ca^{2+} release from ER stores into the cytoplasm, and the subsequent accumulation of Ca^{2+} in the mitochondrial matrix can transiently increase oxidative phosphorylation [10]. However, when Ca^{2+} concentrations are elevated and sustained beyond physiological levels, mitochondrial apoptotic signals are triggered, amplified, and executed [11]. Under these conditions, unresolved ER stress may be detrimental to cell survival [12].

Sarco/endoplasmic reticulum Ca^{2+} ATPase (SERCA) is a key player in the regulation of cytosolic free Ca^{2+} [13]. It performs an essential task in Ca^{2+}-signaling homeostasis by

efficiently re-sequestering cytoplasmic Ca^{2+} into the ER, once the desired physiological response is established [14, 15]. Cytosolic free Ca^{2+} is involved in various processes and plays a crucial role in controlling cellular life-or-death decisions, including selection of the mode of cell death, i.e., apoptosis, necrosis, or autophagy [16, 17]. Ca^{2+}/calmodulin-dependent protein kinase (CaMK) is a multifunctional serine/threonine kinase whose activity is regulated by the Ca^{2+}-calmodulin complex. It is involved in many signaling cascades, including cell survival and death [18-20]. CaMK2 alpha (CaMK2α) plays an important role in Ca^{2+}-dependent apoptosis [20]. As cancer cells reprogram their metabolic processes, there is a significant breach in Ca^{2+}-dependent apoptosis [21, 22], which results in a universal increase in survival capacity. This particular characteristic may be typical of a subpopulation of tumor cells selected in unfavorable metabolic microenvironments, which links metabolic subclonal selection and malignant tumor progression. Here, we show that metabolic stress-resistant *in vitro*-selected CSCs (S-231 cells selected from MDA-MB-231 cells and S-MCF-7 cells selected from MCF-7 cells) avoid Ca^{2+}-induced apoptosis during glucose deprivation. In these cells, the CaMK2α pathway is activated and transcriptionally regulates *SERCA* expression *via* nuclear factor kappa B (NFκB) activation. This allows cells to circumvent cytoplasmic Ca^{2+} overload-induced apoptosis following prolonged glucose deprivation. Furthermore, we demonstrate that a combination of agents, which cause cellular bioenergetic stress and inhibition of SERCA, suppresses *in vivo* cancer growth, suggesting a novel clinical approach for the treatment of CSCs.

MATERIALS AND METHODS

Cell culture

Human breast cancer cell lines MDA-MB-231 and MCF-7 were obtained in May 2007 from the American Type Culture Collection (ATCC) and grown in Roswell Park Memorial Institute (RPMI)-1640 medium with 5% fetal bovine serum (FBS). The identities of all cell lines were validated by short tandem repeat (STR) DNA fingerprinting using the AmpFlSTR Identifier kit, according to the manufacturer's instructions (Applied Biosystems, Foster City, CA, USA; 4322288) at the Characterized Cell Line Core Facility. The STR profiles were compared to known ATCC fingerprints (ATCC.org) and to the Cell Line Integrated Molecular Authentication (CLIMA) database version 0.1.200808 (http://bioinformatics.istge.it/clima/) (Nucleic Acids Research 37:D925-D932 PMCID: PMC2686526). Mycoplasma contamination was invariably checked with Lookout Mycoplasma PCR Detection Kit (Sigma Aldrich, MO, USA; MP0035).

Cell viability assay

Cell viability was measured using the MTT (Roche, Basel, Switzerland; 11465007001) and crystal violet assay. Cells were seeded in 96-well plates at 6×10^3 cells/well and incubated overnight to 80% confluence. Cells were exposed to glucose-deprived conditions or CaMK2α inhibitor treatment; incubated for 0, 12, 24, 36, 48, 60, and 72 h; and cell viability was measured using the MTT reagent at 550 nm, according to the manufacturer's protocol. Briefly, MTT reagent (10 μL) was added to every well (final concentration, 0.5 mg/mL) and the plate was incubated at 37 °C. After 4 h, 100 μL of solubilization solution (10% SDS) was added to each well and the plate was incubated for 24 h. After the solubilization, the formazan dye is quantitated using a scanning multi-well

spectrophotometer (ELISA reader).

Microarray experiments and data analysis

Gene expression data from the cancer cell lines were generated by hybridizing labeled RNAs to Human-6 v2 Expression BeadChips (Illumina, San Diego, CA, USA). Total RNA was isolated from cells harvested after glucose deprivation for the indicated time using the mirVana miRNA Isolation Kit (Ambion Inc., Austin, TX, USA; AM1560), according to the manufacturer's protocol. Biotin-labeled cRNA was prepared using the Illumina Total Prep RNA Amplification Kit (Ambion Inc.). Total RNA (500 ng) was used for the synthesis of cDNA followed by amplification and biotin labeling. Biotinylated cRNA (1.5 μg) per sample was hybridized to an Illumina Human-6 BeadChip v2 microarray and the signal was developed using Amersham fluorolink streptavidin-Cy3 (GE Healthcare Bio-Sciences, Piscataway, NJ, USA). All statistical analysis was performed using R 2.3.0 and BRB Arraytools Version 3.5 (https://brb.nci.nih.gov/BRB-ArrayTools/) with quantile normalization. Further protocol and data analysis details are described in our previous paper [5].

Intracellular calcium concentration measurements

The intracellular free Ca^{2+} concentration was titrated using calcium calibration buffer KIT#1 (Life Technologies, Waltham, MA, USA; C3008MP), according to the manufacturer's protocol. Fluorescence in the presence of different Ca^{2+} and ethylene glycol-bis (β-aminoethyl ether)-N,N,N',N'-tetraacetic acid (EGTA) standard solutions was measured using a fluorophore with the cell suspension. Measurements were performed by mixing 3 μL of purified GCaMP (~100 μM) with 100 μL of different ratios of calcium buffer and 39 μM free-calcium buffer in 96-well transparent plates (Greiner BIO-one, Frickenhausen, Germany) and

measuring the fluorescence at 485 nm excitation and 510 nm emission, with 5 nm slits and gain = 90 V.

Total RNA extraction and quantitative real-time reverse transcription RT-PCR (qRT-PCR)

Total RNA was prepared from tumor cells by extraction with the RNeasy Mini Kit (Qiagen, Valencia, CA, USA; 74106) and the One-Step RT-PCR Kit (Qiagen; 204243) according to the manufacturer's protocols. All data were normalized to the expression level of α tubulin. Primers for *SERCA1, SERCA2,* and *SERCA3* are listed in Supplementary Table S1.

Small interfering RNA (siRNA) transfection for CaMK2α knockdown

CSCs (S-231 and S-MCF-7) were transfected with CaMK2α siRNA or control scrambled siRNA. The sequence of the CaMK2α siRNA was designed using si-Designed software (Bioneer, Daejeon, South Korea) and the siRNA duplex was purchased from Bioneer. The sense and antisense sequences of the siRNA were as follows: 5′-UGAUCGAAGCCAUAAGCAA(dTdT)-3′ (forward) and 5′-UUGCUUAUGGCUUCGAUCA(dTdT)-3′ (reverse).

Evaluation of cell death using TUNEL assay

For the measurement of apoptotic death, cells were fixed with 4% paraformaldehyde for 48 h and stained using a TUNEL Kit (Promega, Madison, WI, USA; G3250). Apoptotic cells (fluorescent green) and total cells were counted under a fluorescence microscope, and the data were recorded. Images were collected using a confocal microscope (LSM Meta 700, Carl Zeiss, Jena, Germany) and were analyzed using the Zeiss LSM Image Browser software

program, version 4.2.0121.

Subcellular fractionation and immunoblot analysis

Antibodies against caspase-3, caspase-7, caspase-9, Bcl-2, Bcl-$_{xL}$, pNFκB, NFκB, Histone H2B, β-actin (all Santa Cruz Biotechnology, Santa Cruz, CA, USA), pCaMK2α, CaMK2α, pIP3R, IP3R, pIKKα, IKKα, and SERCA2 (all Abcam, Cambridge, UK) were used. Nuclear fractions were prepared using the NE-PER® Nuclear and Cytoplasmic Extraction reagents (Thermo Scientific, Rockford, IL, USA; 78833) in accordance with the manufacturer's instructions. Protein bands were quantified using ImageJ software (NIH, Bethesda, MD, USA).

Flow cytometry for cell cycle analysis

Cells were treated with glucose-deprived RPMI-1640 medium with 10% FBS for 40 h, harvested by trypsinization, and fixed with 70% ethanol. Cells were stained for total DNA using a solution containing 40 μg/mL propidium iodide (PI) and 100 μg/mL RNase I in phosphate-buffered saline (PBS) for 30 min at 37 °C. Cell cycle distribution was then analyzed using a FACS Calibur Flow Cytometer (BD Biosciences, Franklin Lakes, NJ, USA). The proportions of cells in the G0/G1, S, and G2/M phases were analyzed using FlowJo v8 software (Tree Star, Ashland, OR, USA). This experiment was repeated three times, and the results were averaged.

Electrophoretic mobility shift assay (EMSA)

The DNA binding of NFκB to the *SERCA2* promoter [23] was investigated using an EMSA with ^{32}P-labeled oligonucleotides and nuclear extracts from parental cells and CSCs.

Nuclear extracts were isolated using NE-PER Nuclear and Cytoplasmic Extraction Reagents (Pierce, Rockford, IL, USA; 78833). The DNA binding activity of NFκB against the *SERCA2* promoter was confirmed using a ^{32}P-labeled oligonucleotide. Labeled and unlabeled oligonucleotides specific for NFκB (Forward 5′-GGGGGGTTCCC-3′, Reverse 5′-GGGAACCCCCC-3′) and mutant NFκB (Forward 5′-GGGcGcTTCCC-3′, Reverse 5′-GGGAAgCgCCC-3′) were synthesized by Bioneer. Nuclear extracts-DNA interactions were carried out in a 30-μL reaction mixture containing 5 μg of nuclear protein extract, 50 mM HEPES (pH 7.8), 300 mM KCl, 1% Igepal, 30% glycerol, 1 mM DTT, 0.02 μg of poly (dI-dC), 0.1 μg of ssDNA, and 20 000 CPM of ^{32}P-radiolabeled oligonucleotide. For the supershift assay, 0.5 μg of anti-NFκB antibodies (Santa Cruz Biotechnology) were added to the mixture of nuclear extracts-DNA and incubated for one additional hour at 4 °C. After incubation for 30 min at room temperature, the nuclear extracts-DNA complexes were resolved by 5% non-denaturing polyacrylamide gel (pre-run for 30 min) electrophoresis at 4 °C in a buffer containing 50 mM Tris, pH 7.9, 40 mM glycine, and 1 mM EDTA, run at 150 V. The gel was placed on Whatman paper, covered with plastic wrap, and dried on a gel dryer at 80 °C for approximately 120 min. The gel was scanned using an Image Reader FLA-7000 scanner (GE Healthcare Bio-Sciences) and quantified using MultiGauge V3.1 software (Fuji photo film Co, Ltd., Tokyo, Japan).

Dual Luciferase Reporter Assay

Promoter activity was evaluated using the Dual-Luciferase Reporter Assay (Promega, Madison, WI, USA; E1960), according to the manufacturer's protocol. Regions of NFκB binding sites were amplified by PCR from human genomic DNA (NFκB primers: Forward 5′-GGGGGGTTCCC-3′, Reverse 5′-GGGAACCCCCC-3′). The PCR products were cloned into

the pGL4.70 promoter Vector (Promega) using T4 DNA ligase (Thermo Scientific, Waltham, MA, USA; EL0011). All insertions were confirmed by sequencing. Cells were co-transfected with a plasmid containing the 3XκB-Luc reporter, as well as with a *Renilla* luciferase in pGL4.70 (as the control). Luciferase detection was carried out 48 h after reporter transfection. Expression was estimated as the relative *Firefly* luciferase activity normalized to the activity of transfection control *Renilla* luciferase.

Immunofluorescence analysis

CSCs were incubated with a CaMK2α inhibitor (KN-62) in 35-mm glass-bottom microwell (14 mm) dishes. Images were observed under a confocal microscope (LSM Meta 700) and were analyzed using the Zeiss LSM Image Browser software, version 4.2.0121

Immunohistochemistry

Immunohistochemical staining was performed using a standard protocol. Tumor tissues were fixed in 10% formaldehyde and were embedded in paraffin. Tissue sections (5 μm) were dewaxed, and antigen retrieval was carried out in citrate buffer (pH 6), with an electric pressure cooker set at 120 °C for 8 min. Sections were incubated for 10 min in 3% hydrogen peroxide to quench endogenous tissue peroxidase. Primary monoclonal antibodies against CaMK2α (Abcam), Bcl-2 (Abcam), and SERCA2 were diluted with PBS at a ratio of 1:100 and incubated overnight at 4 °C. All tissue sections were counterstained with hematoxylin, dehydrated, and mounted.

Image analysis

MetaMorph 4.6 software (Universal Imaging Co., Downington, PA, USA) was used

for computerized quantification of immunostained target proteins.

In vivo mouse xenograft study

Cancer cells were cultured and subcutaneously injected into the mammary fat pads of 5- to 6-week-old BALB/c nude mice (1.0×10^6 cells/mouse). The tumor size was measured every other day using calipers. The tumor volume was estimated using the following formula: $L \times S^2/2$, where L = longest diameter and S = shortest diameter. When the tumor size reached approximately 100–200 mm^3, tumor-bearing mice were randomly grouped (n = 8–9/group) and 2DG (500 mg/kg), thapsigargin (15 mg/kg), or combinations of 2DG + thapsigargin, 2DG + metformin (250 mg/kg), 2DG + metformin + thapsigargin were injected intraperitoneally (i.p.) or *via* oral (p.o.) gavage, once every three days. Animals were maintained under specific pathogen-free (SPF) conditions. All experiments were approved by the Animal Experiment Committee of Yonsei University.

Statistical analysis

Statistical analysis was performed using Prism 6.0 software (GraphPad Software, Inc., San Diego, CA, USA.), Excel (Microsoft Corp., Redmond, CA, USA), and R version 2.17. One-way ANOVA was performed for the multi-group analysis, and two-tailed Student's *t*-test was performed for the two-group analysis.

RESULTS

Metabolic stress-resistant CSCs exhibit increased anti-apoptotic capabilities upon prolonged glucose deprivation

Previously, we demonstrated that adaptation to chronic metabolic stress led to the positive selection of subclones with cancer stem-like characteristics [5]. To evaluate the acquired capability of stress-resistant CSCs against metabolic stress conditions, we assessed cell viability in parental cells and CSCs (derived from both MDA-MB-231 and MCF-7 cells) after exposure to glucose deprivation for 0, 24, 36, 48, or 60 h. Both parental cells (P-231 and P-MCF-7) and CSCs (S-231 and S-MCF-7) exhibited increased apoptotic cell death as the period of glucose deprivation increased (Figure 1A). However, a significant number of CSCs survived even after 60 h of glucose deprivation, whereas most parental cells did not (Figure 1A–D). A 3-(4,5-dimethylthiazol-2-yl)-2,5-diphenyltetrazolium bromide (MTT) assay confirmed these results (Figure 1B).

Given that caspase activation is an indicator of apoptosis, we measured caspase-3, -7, and -9 cleavage (Figure 1C). As MCF-7 cells do not express caspase-3, we measured caspase-9 cleavage instead in these cells. Bcl-2, an anti-apoptotic protein, was also elevated in CSCs compared to that in parental cells following long-term exposure to glucose deprivation (Figure 1C). The terminal deoxynucleotidyl transferase dUTP nick end labeling (TUNEL) assay also revealed more DNA fragmentation, indicating increased apoptosis, in parental cells compared to that in CSCs (Figure 1D). Cell cycle analysis indicated that the number of cells in the sub-G0/G1 phase was greater in the parental cells than in the CSCs after long-term exposure to glucose deprivation (40 h, P-231 29.3% *vs*. S-231 4.4%; P-MCF-7 21.3% *vs*. S-MCF-7 7.5%), whereas this difference was insignificant after short-term exposure (12 h, P-231 1.2% *vs*. S-231 1.1%; P-MCF-7 0.2% *vs*. S-MCF-7 0.2%) (Figure 1E). Taken together,

these data indicated that CSCs exhibit significant resistance to apoptosis upon prolonged glucose deprivation compared with their parental lineages.

CSCs undergo distinct transcriptional reprogramming

Considering that gene expression is largely influenced by signals from the environment, we speculated that CSCs would achieve a stem-like phenotype by transcriptional reprogramming. We performed genome-wide transcriptional profiling of paired P-231 and S-231 samples. A large number of genes were significantly differentially expressed between P-231 and S-231 cells, suggesting that multiple biological processes were reprogrammed in CSCs. Calcium signaling was identified as one of the most significantly over-represented pathways in CSCs by gene set analysis (Figure 2A, Left panel). Considering the distinctive gene expression patterns observed in the presence and absence of glucose across P- and S-cells, the most notable differentially expressed gene was *SERCA2 (ATP2A2)*, which is involved in calcium signaling (Figure 2A, Right panel). Furthermore, the SERCA2 protein level was remarkably increased in CSCs compared to that in parental cells during glucose deprivation (Figure 2B). Cytosolic free calcium levels were lower in CSCs than in parental cells following short- or long-term glucose deprivation (Figure 2C). In contrast, no significant differences in SERCA and cytosolic free calcium levels were observed between parental cells and CSCs at baseline (complete medium) (Figure 2B and C).

Collectively, these results suggested that CSCs survive long-term glucose deprivation by transcriptional reprogramming involving intracellular calcium homeostasis regulatory pathways.

Survival of CSCs upon prolonged glucose deprivation depends on CaMK2α

The release of Ca^{2+} from the ER into the cytosol is an early and crucial event in apoptosis [24, 25]. CaMK2α is regulated by Ca^{2+} and plays an important role against apoptosis [26, 27]. During glucose deprivation, CSCs exhibited increased levels of phosphorylated CaMK2α (pCaMK2α) as well as anti-apoptosis-related Bcl-$_{xL}$ and Bcl-2, while the expression of the channel proteins itself did not differ, but phosphorylated IP3R (pIP3R) was significantly downregulated (Figure 3A). Interestingly, knockdown of *CAMK2A* (encoding CaMK2α) in CSCs (using short interfering RNAs (siRNAs) S-231 si-CaMK2α and S-MCF-7 si-CaMK2α, Figure 3B) led to reduced levels of anti-apoptosis-related protein levels (pIKKα, pNFκB, Bcl-$_{xL}$, and Bcl-2) and SERCA2, but higher levels of pIP3R (Figure 3C). Furthermore, failure to restore basal intracellular Ca^{2+} levels in CSCs (Figure 3D) was accompanied by increased apoptosis after long-term glucose deprivation (Figure 3E and F). On *CAMK2A* knockdown in P-MCF-7 for long-term glucose deprivation, all cells died and hence the release of Ca^{2+} from the ER into the cytosol could not be measured (Figure 3D).

A TUNEL assay revealed that siRNA-mediated knockdown of *CAMK2A* led to more DNA fragmentation compared to that in CSCs without *CAMK2A* knockdown after long-term glucose deprivation (Figure 3E). Knockdown of *CAMK2A* in S-231 and S-MCF-7 cells increased sub-G0/G1 phase cells following long-term glucose deprivation (Figure 3F). These results suggested that CaMK2α-mediated anti-apoptosis might be related to restoration of cytosolic Ca^{2+} levels to the basal state, providing protection in CSCs against prolonged glucose deprivation-induced cell death.

NFκB transcriptionally activates SERCA2 expression during survival in glucose-deprived conditions

Long-term exposure of cancer cells to glucose-deprived conditions causes severe ER stress, which induces mitochondrial Ca^{2+} overload and eventually ER stress-mediated apoptosis [7, 28]. NFκB, a transcriptional activator, acts as an inducible regulator of anti-apoptotic gene expression, thereby controlling the pro-survival response [29]. Moreover, research has shown that NFκB signaling induces Bcl-2, which affects the ER Ca^{2+} store by upregulating *SERCA2* expression [30, 31].

Therefore, we investigated the role of NFκB in CSCs during time-dependent Ca^{2+}-mediated and glucose deprivation-induced apoptosis. Basal levels of anti-apoptosis-related proteins (pCaMK2α, pIKKα, pNFκB, Bcl-$_{xL}$, Bcl-2, and cleaved caspase-3, -7, and -9), pIP3R, and SERCA2 did not significantly differ between CSCs and parental cells following short-term glucose deprivation (Figure 4A). However, pCaMK2α, pIKKα, pNFκB, Bcl-$_{xL}$, Bcl-2, and SERCA2 increased prominently, whereas levels of pIP3R and cleaved caspase-3, -7, and -9 were reduced, in CSCs after long-term glucose deprivation (Figure 4A).

SERCA is one of the main Ca^{2+} transporters and removes Ca^{2+} from the cytoplasm; therefore, we measured the levels of SERCA isoforms. None of the SERCA isoforms were induced in P-231 cells; however, SERCA isoform levels increased in S-231 cells as the length of glucose deprivation increased. Among the three SERCA isoforms, *SERCA2* mRNA showed the most significant induction (Figure 4B), which was confirmed in S-MCF-7 cells in comparison with P-MCF-7 cells.

Given the role of NFκB as a transcriptional regulator of various anti-apoptotic genes during stress conditions, we hypothesized that *SERCA2* would also be a transcriptional target of NFκB. To investigate potential NFκB binding to the *SERCA2* promoter region, an electrophoretic mobility shift assay (EMSA) was carried out in the presence of an anti-NFκB antibody with a ^{32}P-labeled oligonucleotide containing NFκB binding sites found in the

SERCA2 promoter (Figure 4C). Supershift analysis showed significant differences between CSCs and parental cells after short-term glucose deprivation, which were even more pronounced following long-term deprivation (Figure 4D and E).

We next examined NFκB transcriptional activation using an NFκB-luciferase reporter assay system, which contains an NFκB binding site from the *SERCA2* promoter. There was a greater than 2–4-fold increase in relative luciferase activity in both S-231 and S-MCF7 cells, particularly after long-term glucose deprivation, compared to that seen in their parental cells (Figure 4F and G, respectively).

Taken together, these results demonstrated that NFκB induces the transcription of *SERCA2*, as well as other anti-apoptosis-related genes, in CSCs.

NFκB activation and the survival of stress-resistant CSCs are suppressed by inhibition of CaMK2α activity

Compared with parental cells, CSCs showed increased capacity for restoration of intracellular free Ca^{2+} levels after long-term glucose deprivation (as shown in Figure 2C). However, CSCs failed to restore cytosolic Ca^{2+} levels after genetic silencing of CaMK2α (Figure 3D), suggesting a potential link between CaMK2α activity and the intracellular Ca^{2+}-regulating mechanism. As shown in Figure 4, NFκB induces *SERCA2* expression and NFκB activation is induced by CaMK2α [32, 33]. Thus, we hypothesized that inhibition of CaMK2α activity would suppress NFκB activation, *SERCA2* expression, and CSCs survival.

We assessed expression levels of NFκB p65 in the nucleus, a barometer of NFκB activation, and the expression of *SERCA2* after treatment with a CaMK2α inhibitor (KN-62) during glucose deprivation. KN-62 treatment downregulated expression levels of nuclear NFκB p65 compared with that seen in untreated cells (Figure 5A and 5B). Furthermore,

levels of SERCA2 and anti-apoptosis-related proteins in CSCs were remarkably reduced after treatment with the CaMK2α inhibitor during long-term glucose deprivation (Figure 5B), indicating that CaMK2α plays a critical role in NFκB's entry into the nucleus. Consequently, CSCs treated with KN-62 exhibited reduced survival in response to long-term glucose deprivation (Figure 5C).

Collectively, CaMK2α activity is required to translocate NFκB into the nucleus, where it activates the transcription of *SERCA2* and the expression of anti-apoptotic genes such as *BCL2*, thereby promoting the survival of CSCs during prolonged glucose deprivation.

Combined treatment with a SERCA inhibitor and glucose deprivation-mimetic suppresses tumor progression in mouse xenograft tumor models

To investigate the anti-tumor effect of a SERCA inhibitor *in vivo*, we developed mouse xenograft tumor models using parental cells and CSCs. Xenograft tumors with parental cancer cells exhibited significantly reduced tumor volumes and weights compared with those comprising CSCs (Figure 6A and B). Levels of anti-apoptosis proteins (pCaMK2α, pNFκB, Bcl-2), and calcium restoration-related proteins (pIP3R and SERCA2) in tumors comprising CSCs were significantly increased compared with those in tumors comprising parental cells (Figure 6C). Consistent with the *in vitro* results, immunohistochemical analysis revealed much higher levels of CaMK2α, Bcl-2, and SERCA2 in CSCs (S-231 and S-MCF-7)-derived tumor tissues than in parental cell-derived tumors (Figure 6D and E).

After confirming the *in vivo* tumor expression of SERCA2, we treated mice with thapsigargin, a SERCA inhibitor, together with various metabolic stress inducers (Figure 6F–H). Thapsigargin treatment alone did not result in significant suppression of tumor growth in mouse xenografts (Figure 6F). However, when we induced energetic stress on the mouse

xenograft tumors by injecting the metabolic inhibitor 2-deoxy-D-glucose (2DG), mimicking *in vivo* glucose deprivation, or metformin, which suppresses mitochondrial bioenergetics, the combined treatment group (2DG plus metformin or/and thapsigargin) exhibited significantly smaller tumor volumes compared with those of groups receiving control treatment, 2DG, or thapsigargin alone (Figure 6F). Intriguingly, in the parental group, the 2DG + metformin treatment alone resulted in significantly smaller tumor volumes compared to those in the control group. Among CSCs, however, 2DG + metformin treatment had no significant effect on tumor size. Taken together, these results indicated that parental cells are more vulnerable to metabolic stress than CSCs. Notably, a synergistic effect of 2DG, metformin, and thapsigargin caused the greatest tumor shrinkage among the combination treatments in both P-231 and S-231 cells (Figure 6F and G). No evidence of systemic toxicity or treatment-related death was observed in any group. There was also no significant effect on the body weight of mice treated with 2DG, metformin, or thapsigargin alone, or in combination (Figure 6H). Anti-apoptotic and calcium restoration-related proteins were prominently downregulated, while calcium release-related proteins were upregulated in the P-cell xenograft model. In contrast, anti-apoptotic and calcium restoration-related proteins were significantly upregulated in CSCs, while calcium release-related proteins were downregulated (Figure 6I and J). These results may offer a new therapeutic opportunity to treat cancers, especially those comprising CSCs.

DISCUSSION

The metabolic reprogramming of cancer cells has received significant attention recently and is considered an emerging hallmark of cancer [34]. A high level of glycolysis, known as the Warburg effect, to satisfy the elevated needs of tumor cells for biosynthetic precursors, can also render cells exquisitely sensitive to glucose deprivation [34, 35]. Conversely, more malignant cancer cells, such as highly metastatic subclones, have acquired a universal survival capacity and are better equipped than the less malignant cells to cope with nutrient-deprivation [35, 36].

To the best of our knowledge, the present study is the first to demonstrate that CaMK2α plays a critical role in anti-apoptosis by inducing SERCA in CSCs under glucose-deprived conditions. Induction of SERCA, which restores excess cytosolic Ca^{2+} to the ER, is mainly responsible for resistance to glucose deprivation-triggered apoptosis. In addition, increased Bcl-2 expression, induced by CaMK2α, acts with SERCA and contributes to the blocking of Ca^{2+}-dependent apoptosis. All these effects are fine-tuned by CaMK2α, which regulates *SERCA* and *BCL2* expression *via* NFκB activation, thereby maintaining cytoplasmic Ca^{2+} homeostasis under glucose-deprived conditions.

The binding of inhibitor of kappa B (IκB) to NFκB masks the nuclear localization signals of NFκB. Phosphorylation of IκB by IκB kinase (IKK) results in IκB degradation. When IκB is degraded, the nuclear localization domain on NFκB is revealed and NFκB moves to the nucleus. Multiple kinases are reported to phosphorylate and activate IKK, one of which appears to be CaMK2α [27, 37].

Glucose deprivation induces an increase in cytosolic free Ca^{2+} *via* ER stress [7, 38]. The ER is the major storage site for Ca^{2+} in the cell, and mitochondria also play an important role in Ca^{2+} homeostasis. Mitochondria can take up cytosolic Ca^{2+} rapidly, acting as a buffer

when cytosolic free Ca^{2+} is elevated. In the mitochondria, Ca^{2+} enhances substrate uptake, NADH production, and the activities of ATP synthase, pyruvate, isocitrate, and α-ketoglutarate dehydrogenase in the tricarboxylic acid cycle, thus promoting mitochondrial metabolism and ATP production [39, 40]. Intriguingly, this temporary augmentation of respiration through mitochondrial reflexive buffering of cytosolic Ca^{2+} explains the homeostasis mechanisms of cellular bioenergetics in acute and early glucose starvation. However, prolonged cytosolic free Ca^{2+} overload is potentially lethal, as it decreases mitochondrial respiration, leading to a decline in membrane potential, mitochondrial swelling, cytochrome c release, and finally, apoptotic cell death [24, 28, 41]. Thus, enhanced restoration of Ca^{2+} to the ER may explain how CSCs survive sustained glucose deprivation-induced apoptosis.

Some studies have indicated that Bcl-2 might affect mitochondrial Ca^{2+} homeostasis [42, 43], which was first demonstrated in neural cells. In this model, over-expression of *BCL2* allows mitochondria to take up more Ca^{2+} without causing mitochondrial respiratory disorder, indicating that Bcl-2 can protect mitochondria from an excess of Ca^{2+} [44].

In this study, we showed that despite Ca^{2+} overburden in CSCs after long-term glucose deprivation, apoptotic cell death was not triggered, because CSCs increased their capacity to restore calcium levels by upregulating SERCA levels. CaMK2α has been previously reported to modulate cellular Ca^{2+} homeostasis, either directly or by upregulating the expression of SERCA [45]. Pharmacological inhibition or genetic knockdown of CaMK2α in CSCs caused increased cytoplasmic free Ca^{2+} and reduced SERCA expression after long-term glucose deprivation, as well as reduced anti-apoptotic capacity. Thus, the activation of CaMK2α provides a selective advantage to CSCs during long-term glucose deprivation by regulating cytoplasmic free Ca^{2+} levels *via* SERCA, whose transcription is

also induced by CaMK2α-mediated NFκB activation.

Previously, we showed that dual inhibition of the tumor energy pathway by 2DG and metformin was effective against a broad spectrum of cancer cells [46]. Glucose deprivation can directly affect cellular bioenergetics by suppressing ATP production. It is well appreciated that decreased ATP levels leads to cell death; thus, glucose starvation or 2DG treatment can result in synergistic effects when combined with SERCA inhibition, which also receives inputs from multiple upstream signals [47-50] owing to glucose deprivation-induced cellular stress, other than ER stress. Together, these multiple independent and partially inter-dependent cellular processes would exert synergistic effects in inhibiting tumor growth in metabolic stress caused by glucose deprivation. In this study, we recapitulated that 2DG alone did not have significant anti-tumor effects. Consistent with this result, the combined treatment of thapsigargin with 2DG, but not 2DG alone, which mimics glucose deprivation, resulted in significant anti-tumor effects, suppressing tumor growth in mouse xenograft models. Taken together, these results suggested that CaMK2α-mediated induction of SERCA is a central mechanism by which CSCs survive lethal metabolic stress. Clinically, these observations have significant implications for the development of novel combinatorial strategies that target the selective vulnerabilities of highly malignant cells.

ACKNOWLEDGMENTS

We thank Sang Yong Kim for assistance with the confocal microscopy to measure cytosolic calcium concentration and for critical reading of the manuscript.

REFERENCES

1. Yin L, Kharbanda S, Kufe D: **MUC1 oncoprotein promotes autophagy in a survival response to glucose deprivation**. *Int J Oncol* 2009, **34**(6):1691-1699.

2. Wu H, Ding Z, Hu D, Sun F, Dai C, Xie J, Hu X: **Central role of lactic acidosis in cancer cell resistance to glucose deprivation-induced cell death**. *J Pathol* 2012, **227**(2):189-199.

3. Izuishi K, Kato K, Ogura T, Kinoshita T, Esumi H: **Remarkable tolerance of tumor cells to nutrient deprivation: possible new biochemical target for cancer therapy**. *Cancer Res* 2000, **60**(21):6201-6207.

4. Park HR, Tomida A, Sato S, Tsukumo Y, Yun J, Yamori T, Hayakawa Y, Tsuruo T, Shin-ya K: **Effect on tumor cells of blocking survival response to glucose deprivation**. *J Natl Cancer Inst* 2004, **96**(17):1300-1310.

5. Lee E, Yang J, Ku M, Kim NH, Park Y, Park CB, Suh JS, Park ES, Yook JI, Mills GB *et al*: **Metabolic stress induces a Wnt-dependent cancer stem cell-like state transition**. *Cell death & disease* 2015, **6**:e1805.

6. Lee J, Kee HJ, Min S, Park KC, Park S, Hwang TH, Ryu DH, Hwang GS, Cheong JH: **Integrated omics-analysis reveals Wnt-mediated NAD+ metabolic reprogramming in cancer stem-like cells**. *Oncotarget* 2016, **7**(30):48562-48576.

7. Kim I, Xu W, Reed JC: **Cell death and endoplasmic reticulum stress: disease relevance and therapeutic opportunities**. *Nat Rev Drug Discov* 2008, **7**(12):1013-1030.

8. Orrenius S, Zhivotovsky B, Nicotera P: **Regulation of cell death: the calcium-apoptosis link**. *Nat Rev Mol Cell Biol* 2003, **4**(7):552-565.

9. Ermak G, Davies KJ: **Calcium and oxidative stress: from cell signaling to cell**

death. *Mol Immunol* 2002, **38**(10):713-721.

10. Deniaud A, Sharaf el dein O, Maillier E, Poncet D, Kroemer G, Lemaire C, Brenner C: **Endoplasmic reticulum stress induces calcium-dependent permeability transition, mitochondrial outer membrane permeabilization and apoptosis**. *Oncogene* 2008, **27**(3):285-299.

11. Giorgi C, Baldassari F, Bononi A, Bonora M, De Marchi E, Marchi S, Missiroli S, Patergnani S, Rimessi A, Suski JM *et al*: **Mitochondrial Ca(2+) and apoptosis**. *Cell Calcium* 2012, **52**(1):36-43.

12. Xu C, Bailly-Maitre B, Reed JC: **Endoplasmic reticulum stress: cell life and death decisions**. *J Clin Invest* 2005, **115**(10):2656-2664.

13. Brini M, Carafoli E: **Calcium pumps in health and disease**. *Physiol Rev* 2009, **89**(4):1341-1378.

14. Periasamy M, Huke S: **SERCA pump level is a critical determinant of Ca(2+)homeostasis and cardiac contractility**. *J Mol Cell Cardiol* 2001, **33**(6):1053-1063.

15. Arbabian A, Brouland JP, Gelebart P, Kovacs T, Bobe R, Enouf J, Papp B: **Endoplasmic reticulum calcium pumps and cancer**. *Biofactors* 2011, **37**(3):139-149.

16. Ma Y, Hendershot LM: **ER chaperone functions during normal and stress conditions**. *J Chem Neuroanat* 2004, **28**(1-2):51-65.

17. VanHouten J, Sullivan C, Bazinet C, Ryoo T, Camp R, Rimm DL, Chung G, Wysolmerski J: **PMCA2 regulates apoptosis during mammary gland involution and predicts outcome in breast cancer**. *Proc Natl Acad Sci U S A* 2010, **107**(25):11405-11410.

18. Wang YY, Zhao R, Zhe H: **The emerging role of CaMKII in cancer**. *Oncotarget* 2015, **6**(14):11725-11734.

19. Chai S, Xu X, Wang Y, Zhou Y, Zhang C, Yang Y, Yang Y, Xu H, Xu R, Wang K: **Ca2+/calmodulin-dependent protein kinase IIgamma enhances stem-like traits and tumorigenicity of lung cancer cells**. *Oncotarget* 2015, **6**(18):16069-16083.

20. Rokhlin OW, Taghiyev AF, Bayer KU, Bumcrot D, Koteliansk VE, Glover RA, Cohen MB: **Calcium/calmodulin-dependent kinase II plays an important role in prostate cancer cell survival**. *Cancer Biol Ther* 2007, **6**(5):732-742.

21. Gaude E, Frezza C: **Defects in mitochondrial metabolism and cancer**. *Cancer Metab* 2014, **2**:10.

22. Monteith GR, Davis FM, Roberts-Thomson SJ: **Calcium channels and pumps in cancer: changes and consequences**. *J Biol Chem* 2012, **287**(38):31666-31673.

23. Wong D, Teixeira A, Oikonomopoulos S, Humburg P, Lone IN, Saliba D, Siggers T, Bulyk M, Angelov D, Dimitrov S *et al*: **Extensive characterization of NF-kappaB binding uncovers non-canonical motifs and advances the interpretation of genetic functional traits**. *Genome Biol* 2011, **12**(7):R70.

24. Mattson MP, Chan SL: **Calcium orchestrates apoptosis**. *Nat Cell Biol* 2003, **5**(12):1041-1043.

25. Dejeans N, Tajeddine N, Beck R, Verrax J, Taper H, Gailly P, Calderon PB: **Endoplasmic reticulum calcium release potentiates the ER stress and cell death caused by an oxidative stress in MCF-7 cells**. *Biochem Pharmacol* 2010, **79**(9):1221-1230.

26. Vila-Petroff M, Salas MA, Said M, Valverde CA, Sapia L, Portiansky E, Hajjar RJ, Kranias EG, Mundina-Weilenmann C, Mattiazzi A: **CaMKII inhibition protects**

against necrosis and apoptosis in irreversible ischemia-reperfusion injury. *Cardiovasc Res* 2007, **73**(4):689-698.

27. Rodriguez-Mora O, LaHair MM, Howe CJ, McCubrey JA, Franklin RA: **Calcium/calmodulin-dependent protein kinases as potential targets in cancer therapy**. *Expert Opin Ther Targets* 2005, **9**(4):791-808.

28. Pinton P, Giorgi C, Siviero R, Zecchini E, Rizzuto R: **Calcium and apoptosis: ER-mitochondria Ca2+ transfer in the control of apoptosis**. *Oncogene* 2008, **27**(50):6407-6418.

29. Catz SD, Johnson JL: **Transcriptional regulation of bcl-2 by nuclear factor kappa B and its significance in prostate cancer**. *Oncogene* 2001, **20**(50):7342-7351.

30. Kuo TH, Kim HR, Zhu L, Yu Y, Lin HM, Tsang W: **Modulation of endoplasmic reticulum calcium pump by Bcl-2**. *Oncogene* 1998, **17**(15):1903-1910.

31. Rong Y, Distelhorst CW: **Bcl-2 protein family members: versatile regulators of calcium signaling in cell survival and apoptosis**. *Annu Rev Physiol* 2008, **70**:73-91.

32. Ishiguro K, Green T, Rapley J, Wachtel H, Giallourakis C, Landry A, Cao Z, Lu N, Takafumi A, Goto H *et al*: **Ca2+/calmodulin-dependent protein kinase II is a modulator of CARMA1-mediated NF-kappaB activation**. *Mol Cell Biol* 2006, **26**(14):5497-5508.

33. Meffert MK, Chang JM, Wiltgen BJ, Fanselow MS, Baltimore D: **NF-kappa B functions in synaptic signaling and behavior**. *Nat Neurosci* 2003, **6**(10):1072-1078.

34. Graham NA, Tahmasian M, Kohli B, Komisopoulou E, Zhu M, Vivanco I, Teitell MA, Wu H, Ribas A, Lo RS *et al*: **Glucose deprivation activates a metabolic and signaling amplification loop leading to cell death**. *Mol Syst Biol* 2012, **8**:589.

35. Cantor JR, Sabatini DM: **Cancer cell metabolism: one hallmark, many faces**.

Cancer Discov 2012, **2**(10):881-898.

36. Vidal SJ, Rodriguez-Bravo V, Galsky M, Cordon-Cardo C, Domingo-Domenech J: **Targeting cancer stem cells to suppress acquired chemotherapy resistance**. *Oncogene* 2014, **33**(36):4451-4463.

37. Yano S, Tokumitsu H, Soderling TR: **Calcium promotes cell survival through CaM-K kinase activation of the protein-kinase-B pathway**. *Nature* 1998, **396**(6711):584-587.

38. Wang C, Nguyen HN, Maguire JL, Perry DC: **Role of intracellular calcium stores in cell death from oxygen-glucose deprivation in a neuronal cell line**. *J Cereb Blood Flow Metab* 2002, **22**(2):206-214.

39. Tarasov AI, Griffiths EJ, Rutter GA: **Regulation of ATP production by mitochondrial Ca(2+)**. *Cell Calcium* 2012, **52**(1):28-35.

40. Nguyen MH, Jafri MS: **Mitochondrial calcium signaling and energy metabolism**. *Ann N Y Acad Sci* 2005, **1047**:127-137.

41. Gao LL, Li FR, Jiao P, Yao ST, Sang H, Si YH: **Apoptosis of human ovarian cancer cells induced by Paris chinensis dioscin *via* a Ca(2+)-mediated mitochondrion pathway**. *Asian Pac J Cancer Prev* 2011, **12**(5):1361-1366.

42. Zhu L, Ling S, Yu XD, Venkatesh LK, Subramanian T, Chinnadurai G, Kuo TH: **Modulation of mitochondrial Ca(2+) homeostasis by Bcl-2**. *J Biol Chem* 1999, **274**(47):33267-33273.

43. Bonneau B, Prudent J, Popgeorgiev N, Gillet G: **Non-apoptotic roles of Bcl-2 family: the calcium connection**. *Biochim Biophys Acta* 2013, **1833**(7):1755-1765.

44. Murphy AN, Bredesen DE, Cortopassi G, Wang E, Fiskum G: **Bcl-2 potentiates the maximal calcium uptake capacity of neural cell mitochondria**. *Proc Natl Acad*

Sci U S A 1996, **93**(18):9893-9898.

45. Traister A, Li M, Aafaqi S, Lu M, Arab S, Radisic M, Gross G, Guido F, Sherret J, Verma S *et al*: **Integrin-linked kinase mediates force transduction in cardiomyocytes by modulating SERCA2a/PLN function**. *Nat Commun* 2014, **5**:4533.

46. Cheong JH, Park ES, Liang J, Dennison JB, Tsavachidou D, Nguyen-Charles C, Wa Cheng K, Hall H, Zhang D, Lu Y *et al*: **Dual inhibition of tumor energy pathway by 2-deoxyglucose and metformin is effective against a broad spectrum of preclinical cancer models**. *Mol Cancer Ther* 2011, **10**(12):2350-2362.

47. Ribadeau Dumas A, Wisnewsky C, Boheler KR, Ter Keurs H, Fiszman MY, Schwartz K: **The sarco(endo)plasmic reticulum Ca(2+)-ATPase gene is regulated at the transcriptional level during compensated left ventricular hypertrophy in the rat**. *Comptes rendus de l'Academie des sciences Serie III, Sciences de la vie* 1997, **320**(12):963-969.

48. Aoyagi T, Yonekura K, Eto Y, Matsumoto A, Yokoyama I, Sugiura S, Momomura S, Hirata Y, Baker DL, Periasamy M: **The sarcoplasmic reticulum Ca2+-ATPase (SERCA2) gene promoter activity is decreased in response to severe left ventricular pressure-overload hypertrophy in rat hearts**. *Journal of molecular and cellular cardiology* 1999, **31**(4):919-926.

49. Wankerl M, Boheler KR, Fiszman MY, Schwartz K: **Molecular cloning and analysis of the human cardiac sarco(endo)plasmic reticulum Ca(2+)-ATPase (SERCA2) gene promoter**. *Journal of molecular and cellular cardiology* 1996, **28**(10):2139-2150.

50. Liang CP, Han S, Li G, Tabas I, Tall AR. **Impaired MEK signaling and SERCA**

expression promote ER stress and apoptosis in insulin-resistant macrophages and are reversed by exenatide treatment. *Diabetes* 2012;**61**:2609-2620.

FIGURE LEGENDS

Figure 1. Cell viability of parental and CSC (S-231, S-MCF-7) cells during glucose deprivation. A, Morphological analysis of parental cells and CSCs during glucose deprivation. Scale bar, 80 μm. Morphological analysis was performed in triplicates and representative images are displayed. The cell viability was quantified by crystal violet assay. B, Cell viability assay (MTT) following short- (12 h) and long-term (40 h) exposure to glucose deprivation. C, Immunoblot analysis for caspase-3, -7, and -9, and Bcl-2 after long-term (40 h) exposure to glucose deprivation. D, TUNEL assay after long-term (40 h) exposure to glucose deprivation. TUNEL-positive (apoptotic) cells were examined at 400× magnification. Scale bar, 20 μm. The TUNEL assay was performed in triplicate on different days and representative images are displayed. E, Flow cytometry analysis after short- (12 h) and long-term (40 h) exposure to glucose deprivation. * $P < 0.05$ *vs*. parental, ** $P < 0.01$ *vs*. parental.

Figure 2. Stress-resistant CSCs survive prolonged glucose deprivation by transcriptional reprogramming of cytosolic calcium regulatory pathway genes. A, Unsupervised enrichment plots of parental cells and CSCs using Gene Set Enrichment Analysis (P; parental, S; stem-like cancer cells). Gene set analysis of Kyoto Encyclopedia of Genes and Genomes pathways identified the functional categories of gene sets that were differentially expressed between parental and CSCs. Heat map of the calcium signaling pathway. Hierarchical clustering analysis of genes showed significant differences between P-231 and S-231 cells in the presence or absence (-glu) of glucose. B, Immunoblot analysis of SERCA2 levels in parental cells and CSCs after short- (12 h) and long-term (40 h) exposure to glucose deprivation. C, Cytoplasmic free Ca^{2+} was measured in parental and CSCs after short- (12 h) and long-term (40 h) exposure to glucose deprivation. ** $P < 0.01$ *vs*. parental.

Figure 3. CSCs survival is dependent on CaMK2α under prolonged glucose deprivation. A, Immunoblot analysis of key proteins in the calcium pathway in CSCs compared to their levels in parental cells during glucose deprivation. B and C, Immunoblot analysis for anti-apoptosis-related and calcium restoration-related proteins in CaMK2α-silenced CSCs under long-term (40 h) glucose deprivation conditions. D, Cytoplasmic free Ca^{2+} was measured in CaMK2α-silenced CSCs under short- (12 h) and long-term (40 h) glucose-deprived conditions. E, TUNEL assay after CaMK2α siRNA transfection of CSCs following long-term (40 h) exposure to glucose deprivation. Scale bar, 20 μm. The TUNEL assay was performed in triplicate on different days and representative images are displayed. F, Flow cytometry analysis after silencing of CaMK2α in CSCs. ** $P < 0.01$ *vs*. control.

Figure 4. CaMK2α transcriptionally regulates *SERCA2* expression *via* NFκB under prolonged glucose deprivation conditions. A, Immunoblot analysis of anti-apoptosis- and calcium restoration-related proteins demonstrating time-dependent expression during glucose deprivation. B, qRT-PCR of parental cells and CSCs showing the time-dependent mRNA expression of SERCA family genes during glucose deprivation. C, NFκB binding sites and consensus sequences in the *SERCA2* promoter. D and E, EMSA was performed using nuclear extracts prepared from MDA-MB-231 (D) and MCF-7 (E) cells. F and G, the NFκB-luciferase reporter system was used to compare NFκB transcriptional activity between P- and S- cells (F, MDA-MB231; G, MCF-7 cells). Relative luciferase activity was presented as a readout of NFκB activity. Values of samples were normalized to *Renilla* luciferase. Data represent the average of at least three separate independent experiments, with the standard deviation indicated. * $P < 0.05$, ** $P < 0.01$ *vs*. control or parental.

Figure 5. CaMK2α activity is crucial for NFκB nuclear translocation, SERCA2 expression, and cell survival. A, Immunofluorescence visualization of NFκB in the nucleus

of CSCs after treatment with KN-62, a CaMK2α inhibitor, during long-term (40 h) glucose deprivation conditions. Scale bar, 12.5 μm. Immunofluorescence staining was performed in triplicate on different days and representative images are displayed. B, Immunoblot analysis of anti-apoptosis- and calcium restoration-related proteins in CSCs after long-term (40 h) exposure to glucose deprivation. C, Cell viability assay after short- (12 h) and long-term (40 h) exposure to glucose deprivation in CSCs treated with KN-62. * $P < 0.05$ *vs*. control, ** $P < 0.01$ *vs*. control.

Figure 6. CSCs express higher levels of anti-apoptosis-related and calcium restoration-related proteins than parental cells *in vivo*. Thapsigargin suppresses tumor growth in mouse xenograft models under energy stress conditions. A and B, Changes in relative tumor volumes and weights of parental cells and CSCs (each group, n = 8). Data are presented as means±SEM. C, Immunoblot analysis in tumors derived from parental cells and CSCs. D and E, Immunohistochemical analysis of CaMK2α, Bcl-2, and SERCA2 protein levels in paraffin-embedded xenograft tumor tissues derived from 231 (D) or MCF-7 (E) cells. Scale bar, 80 μm. F and G, Changes in tumor volumes and weights of parental cells and CSCs. F, Tumors were established in athymic nude mice and treated with 2DG, metformin, and thapsigargin, alone or in combination (control group, n = 8; treatment group, n = 9). Data are presented as means±SEM. G, Tumor weight of dissected tumors in (F). H, No evidence of systemic toxicity or treatment-related death was found in any group. I, Immunoblot analysis of anti-apoptotic and calcium related proteins in tumor tissues derived from parental and CSCs. J, Immunohistochemical analysis for Bcl-2, and SERCA2 proteins in tumor tissues according to the indicated treatments. Each assay was performed in triplicate and representative images are displayed. * $P < 0.05$ *vs*. control, ** $P < 0.01$ *vs*. control.

Figure 1

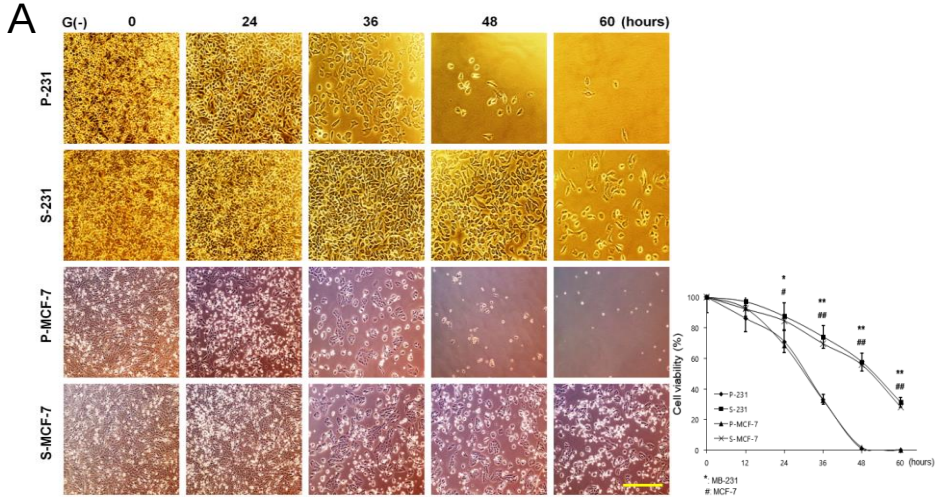

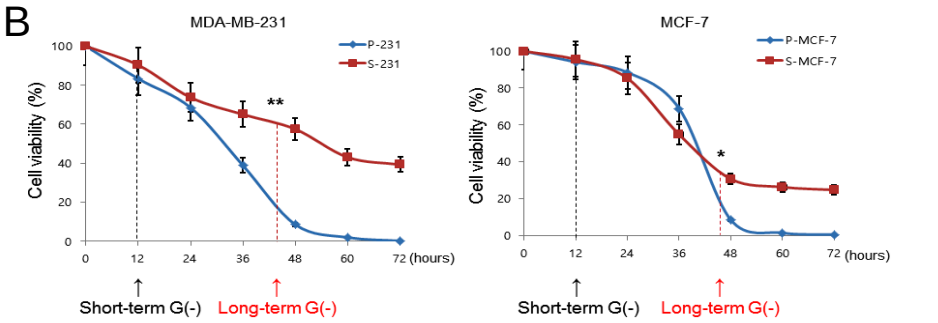

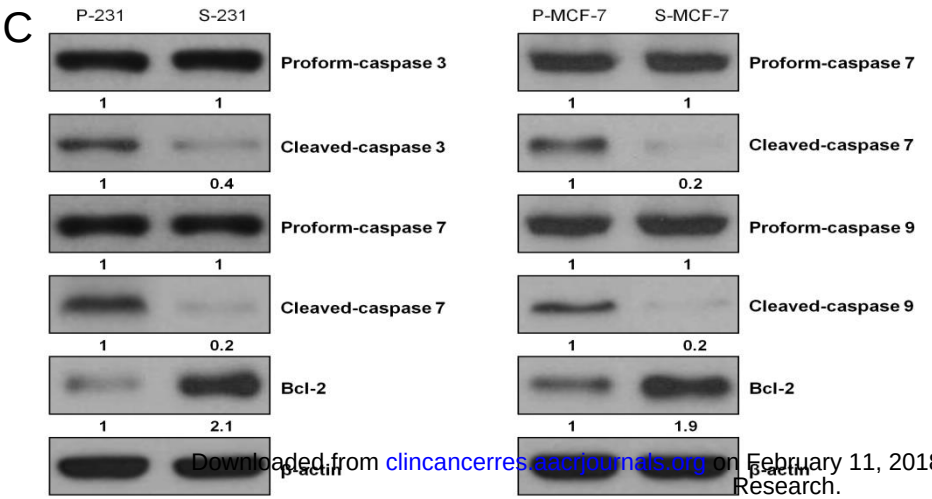

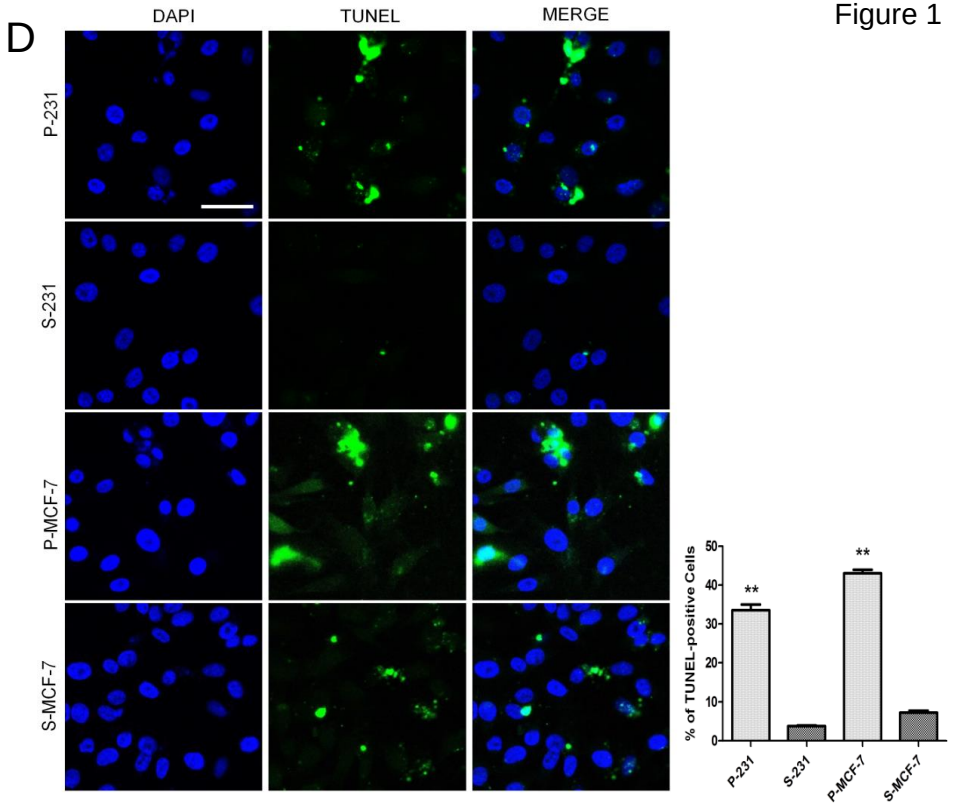

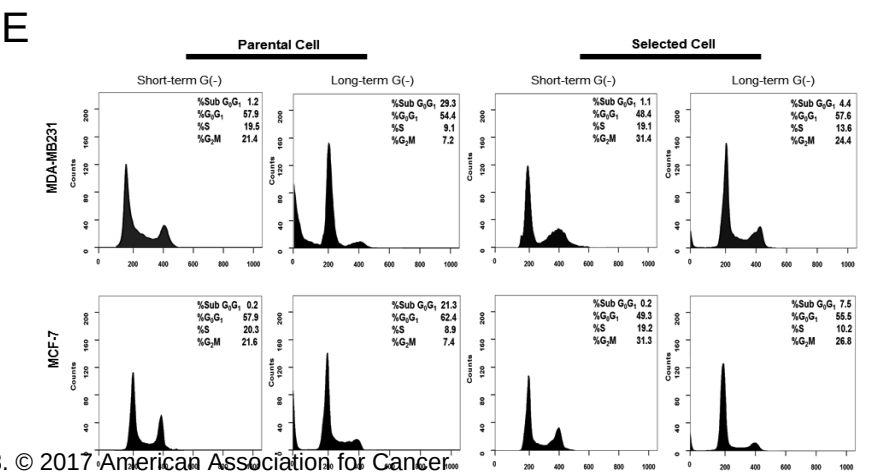

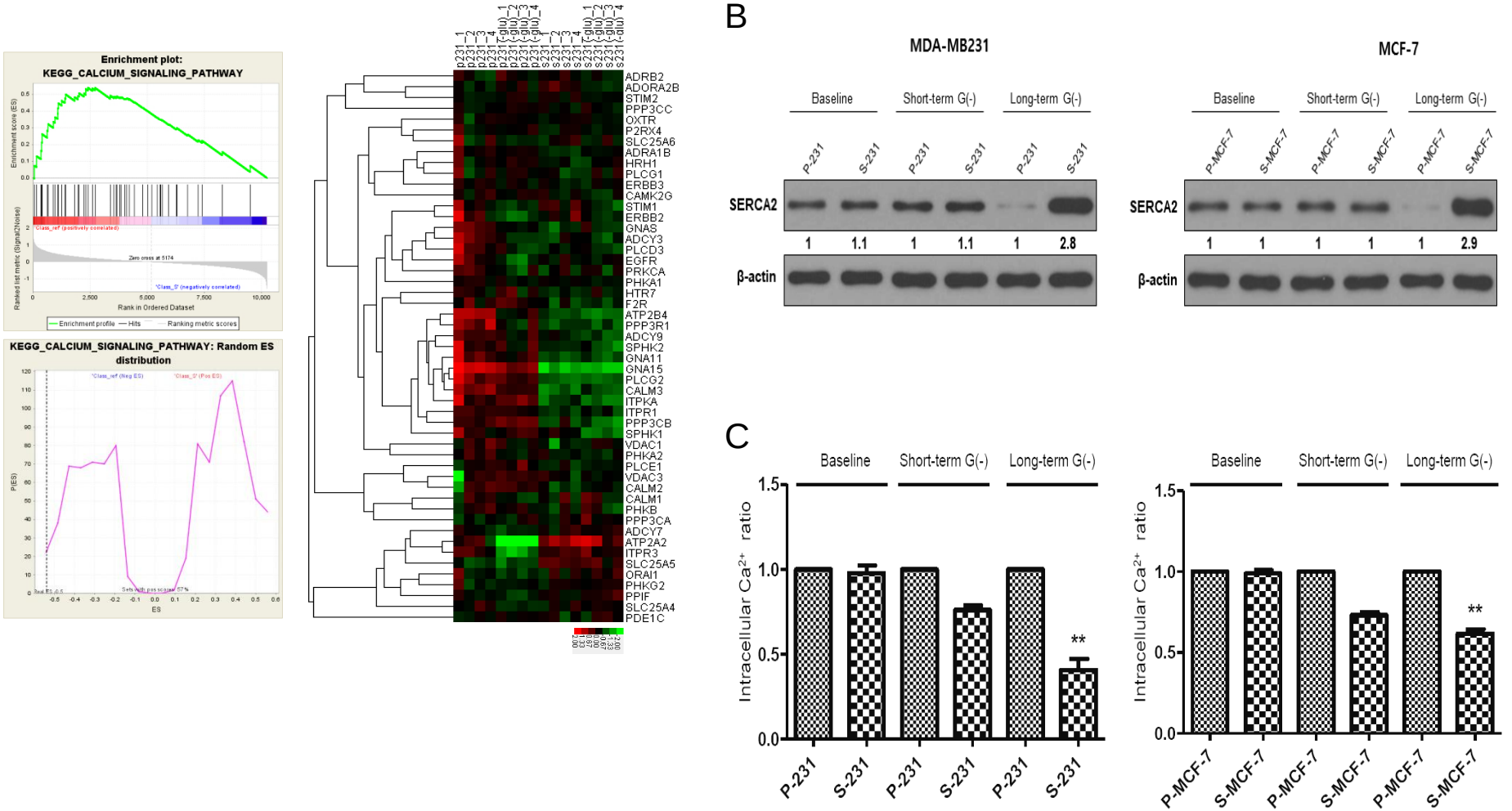

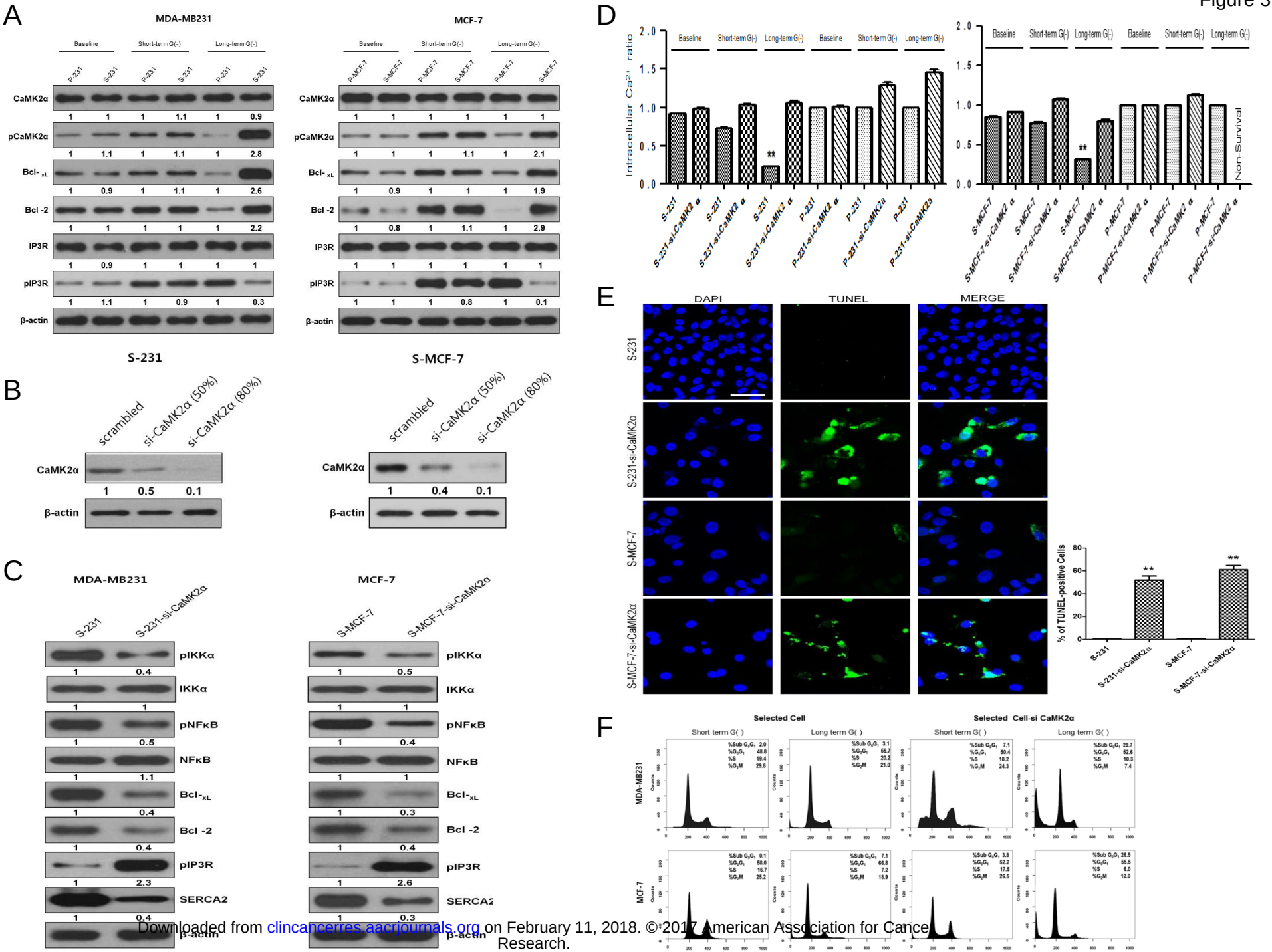

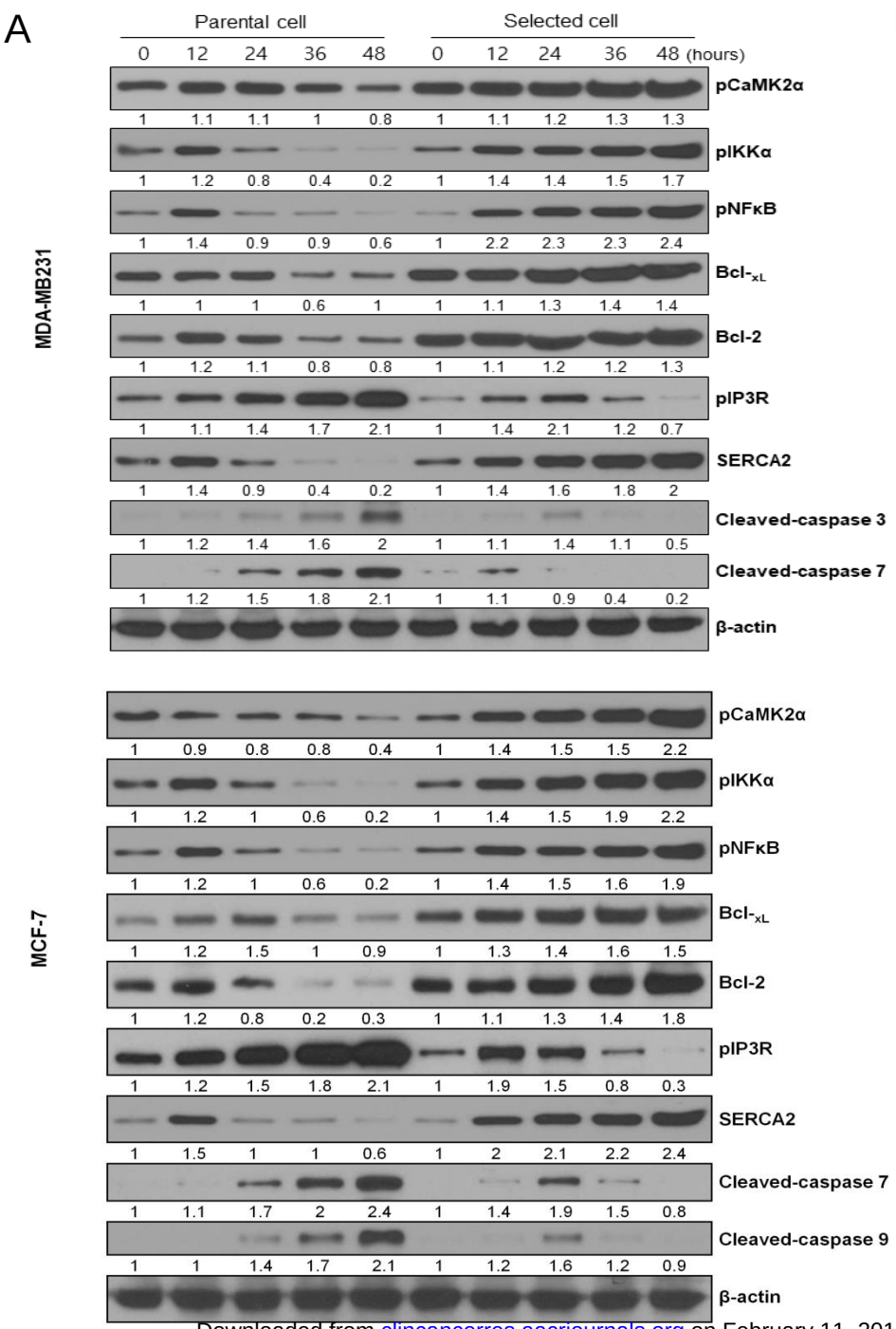

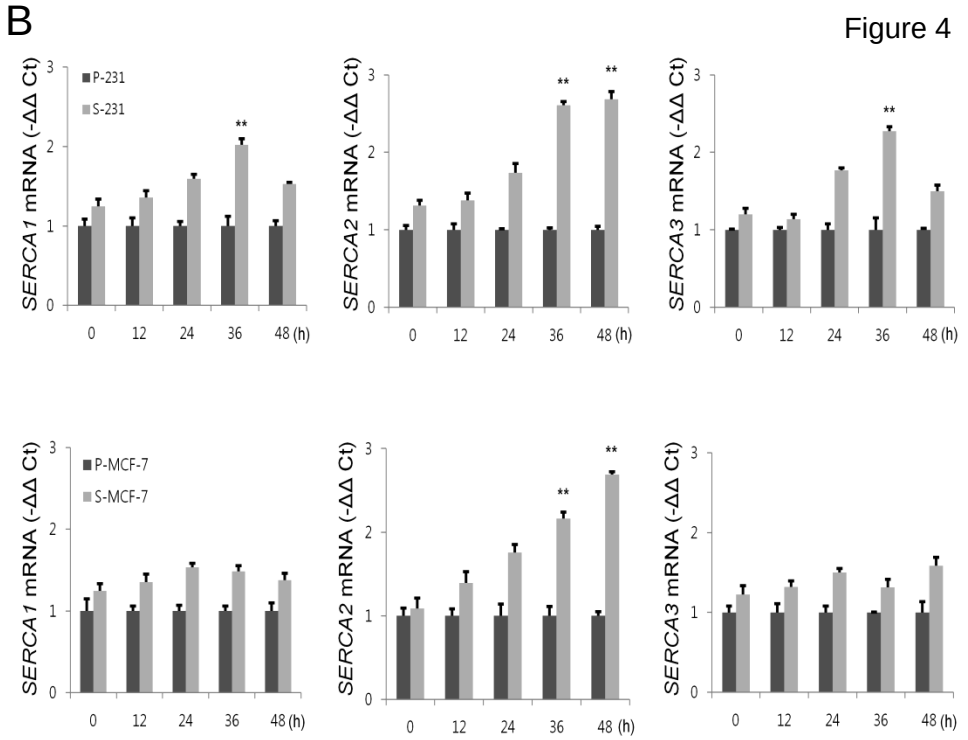

C

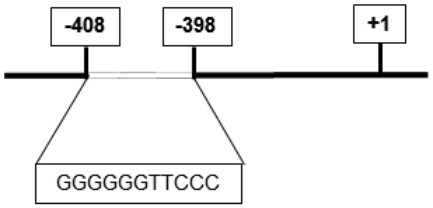

D

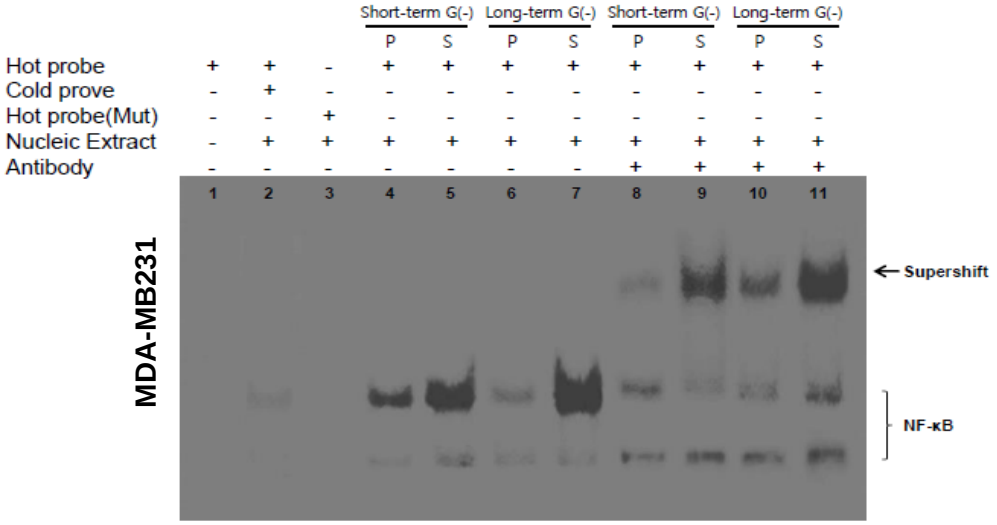

E

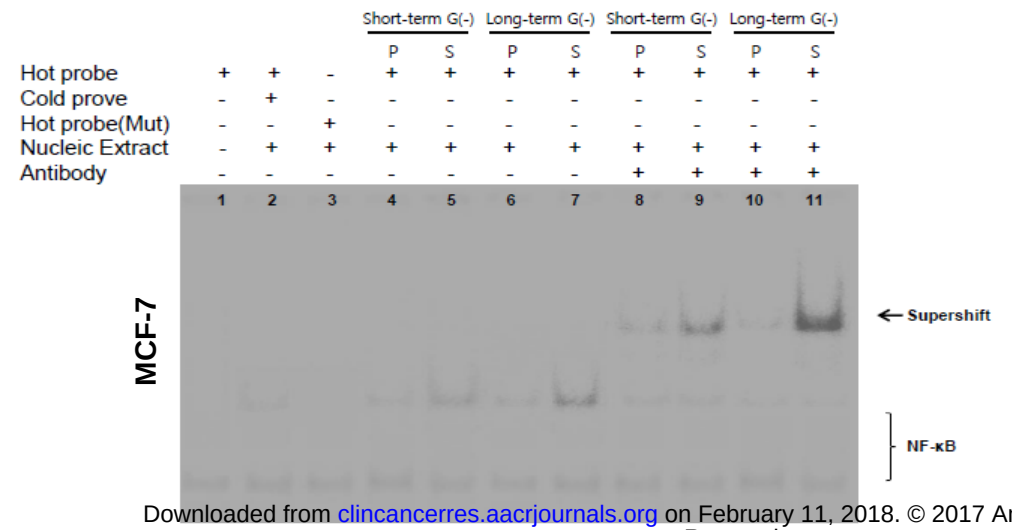

F

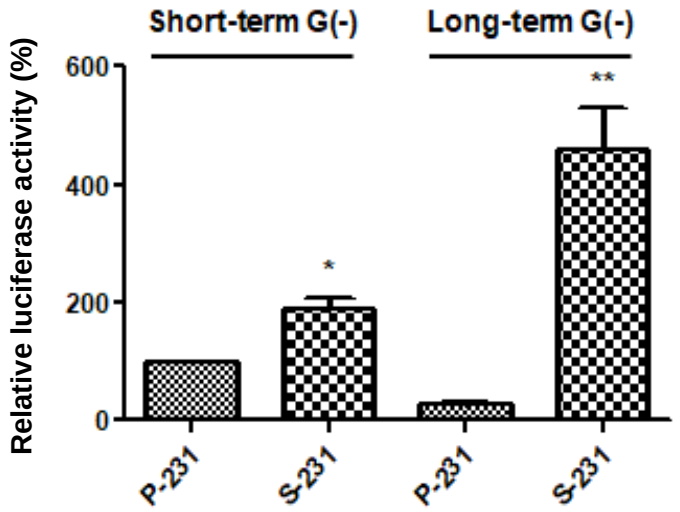

G

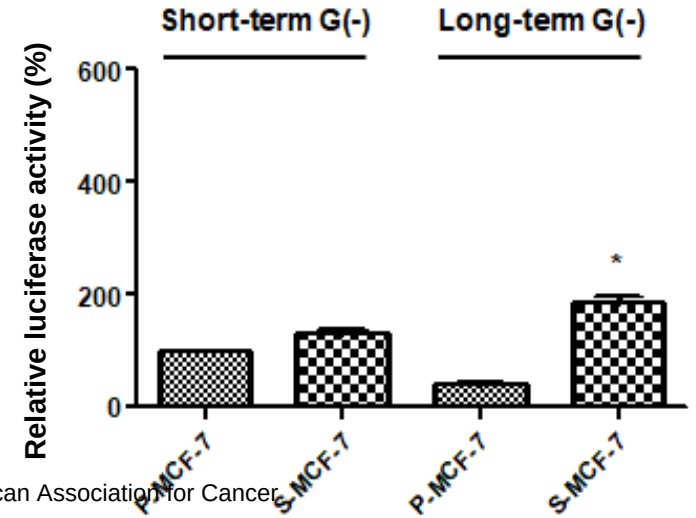

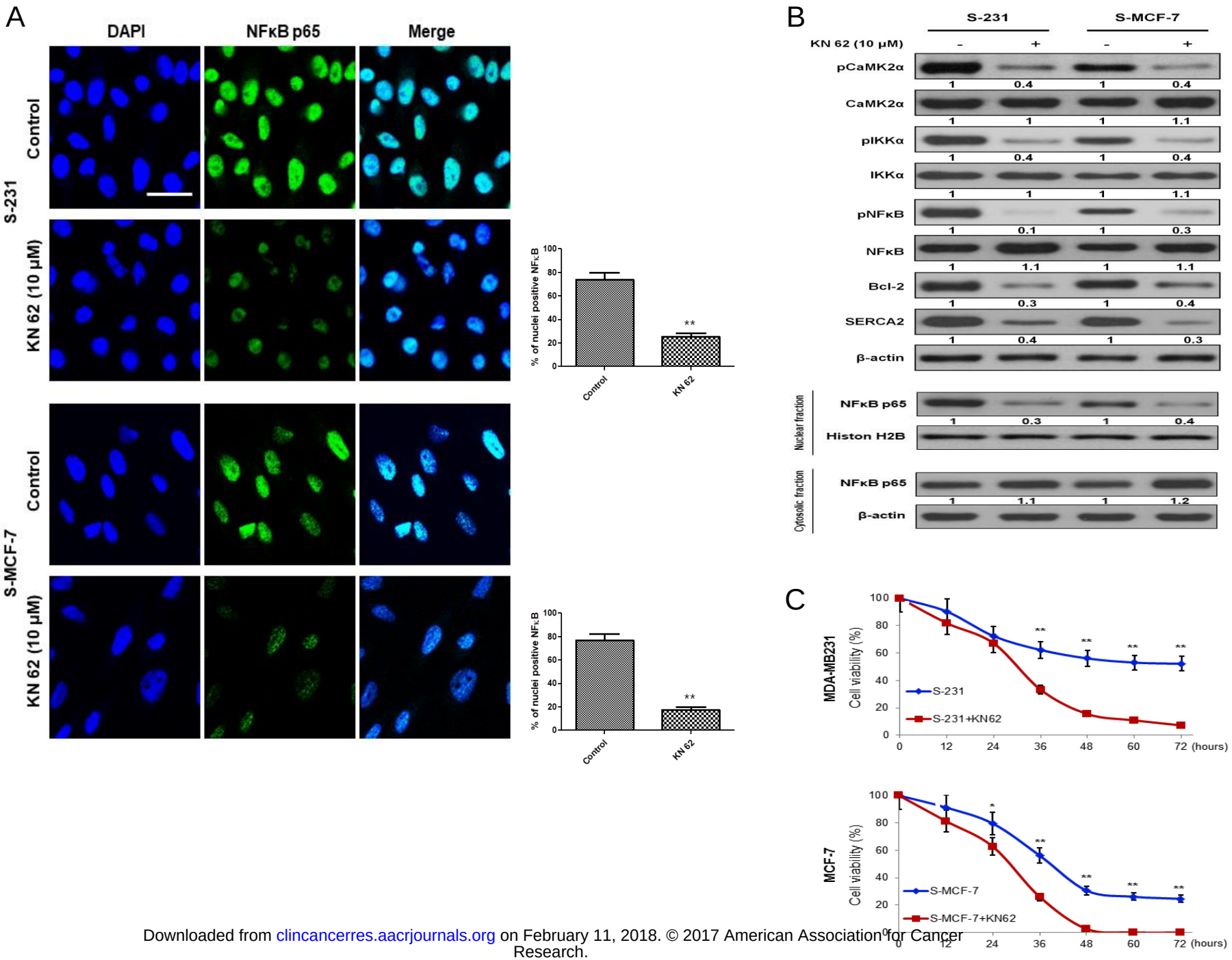

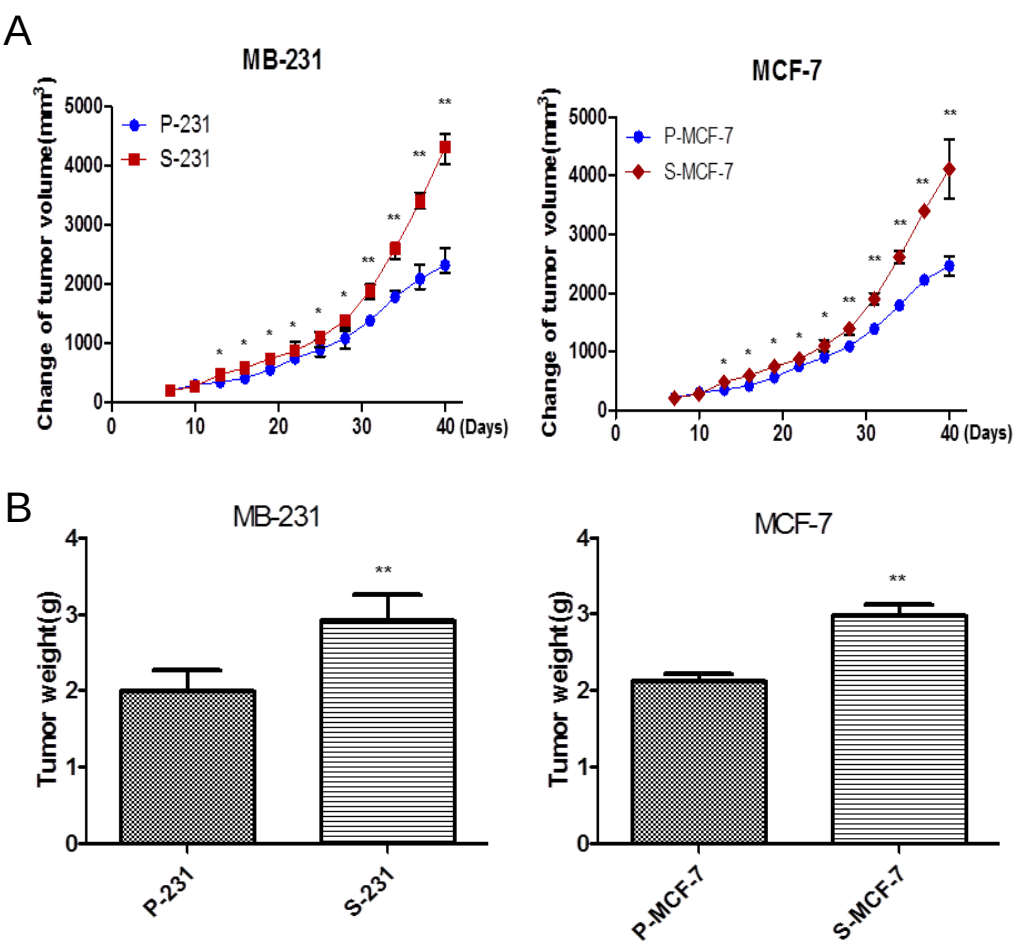

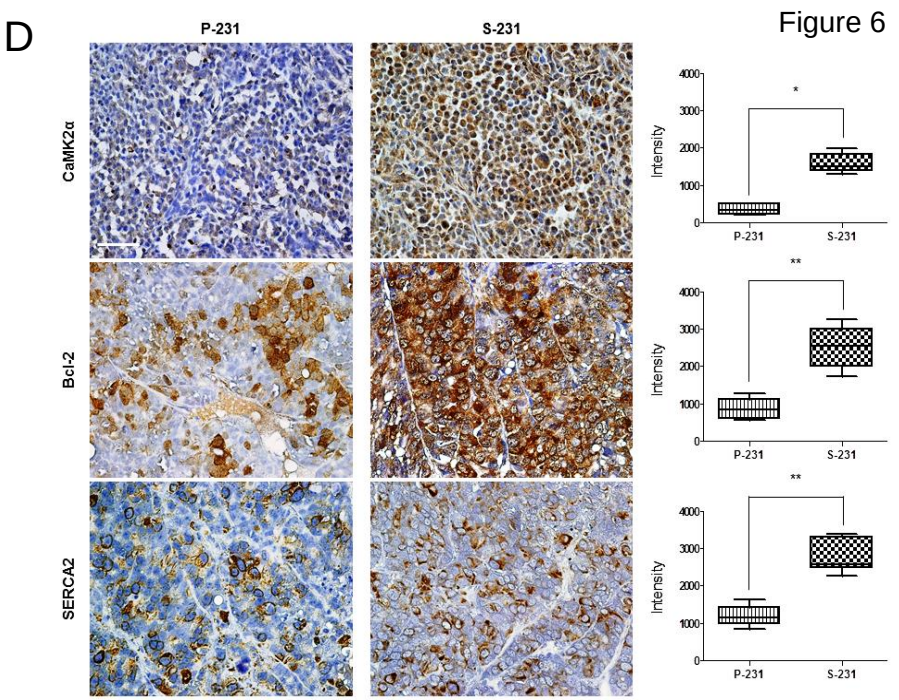

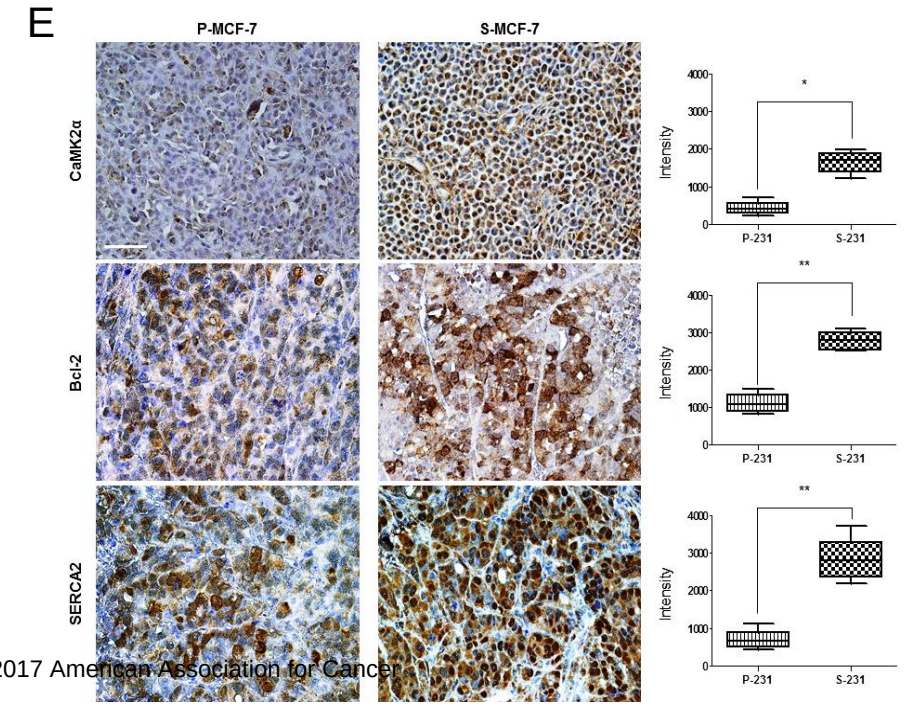

F

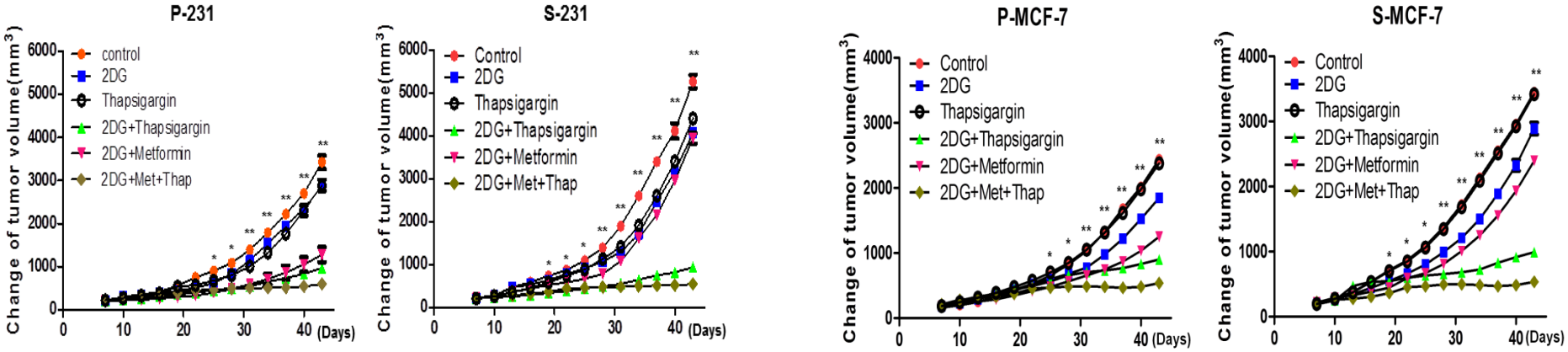

G

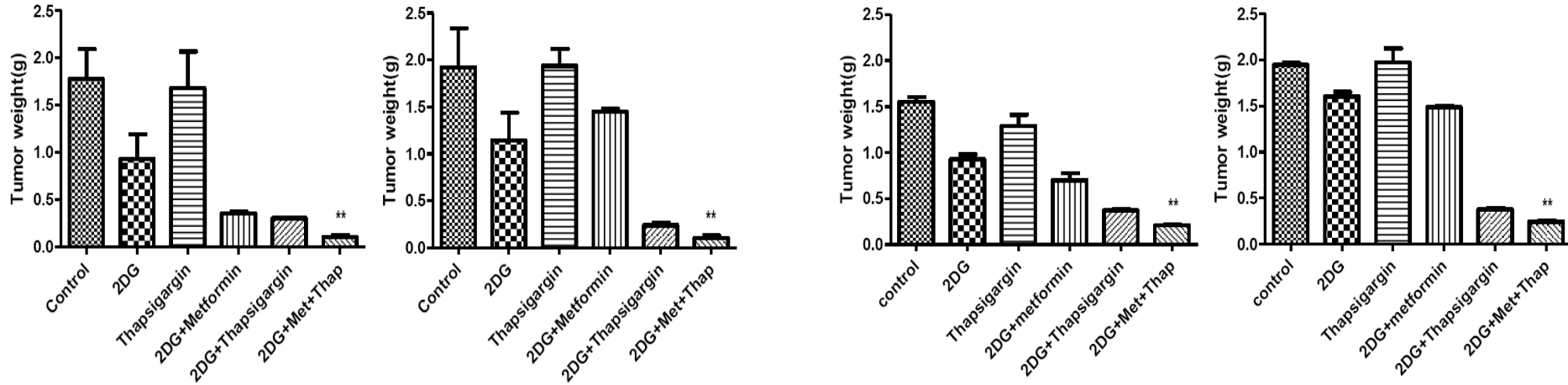

H

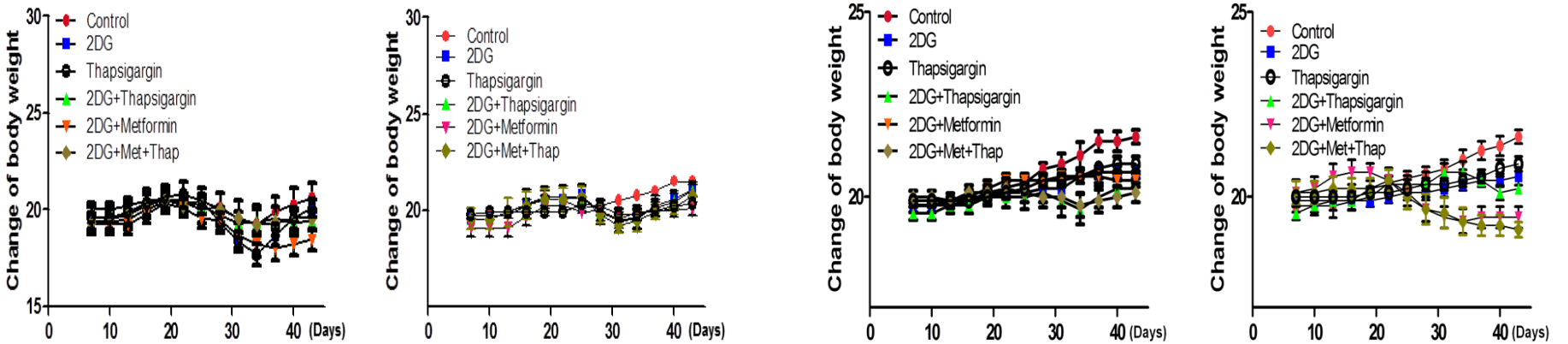

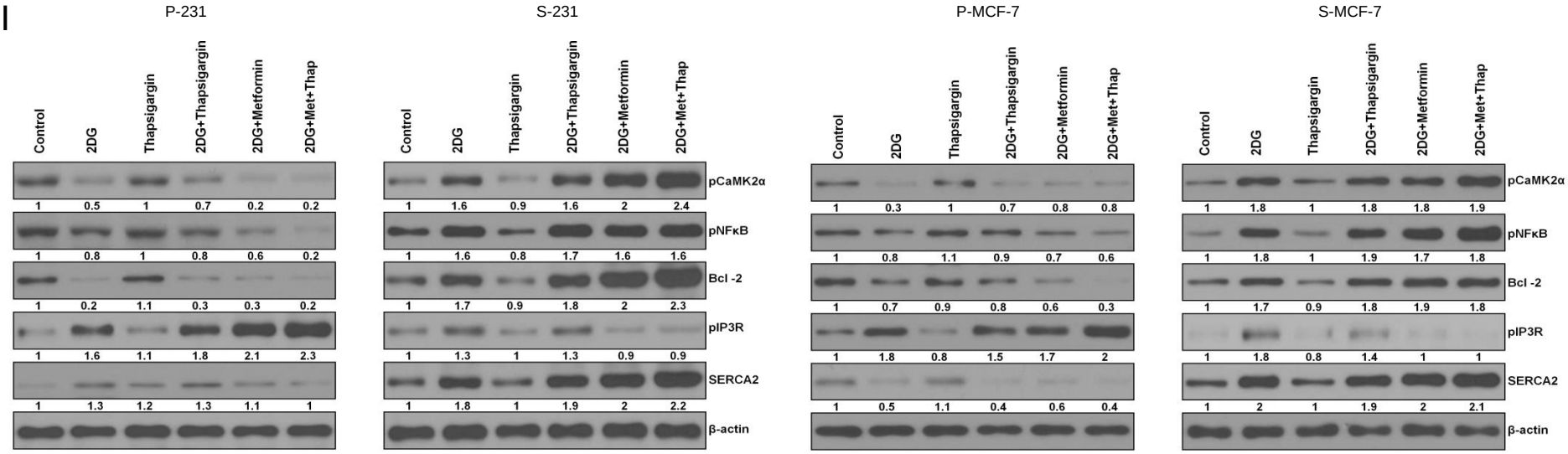

J

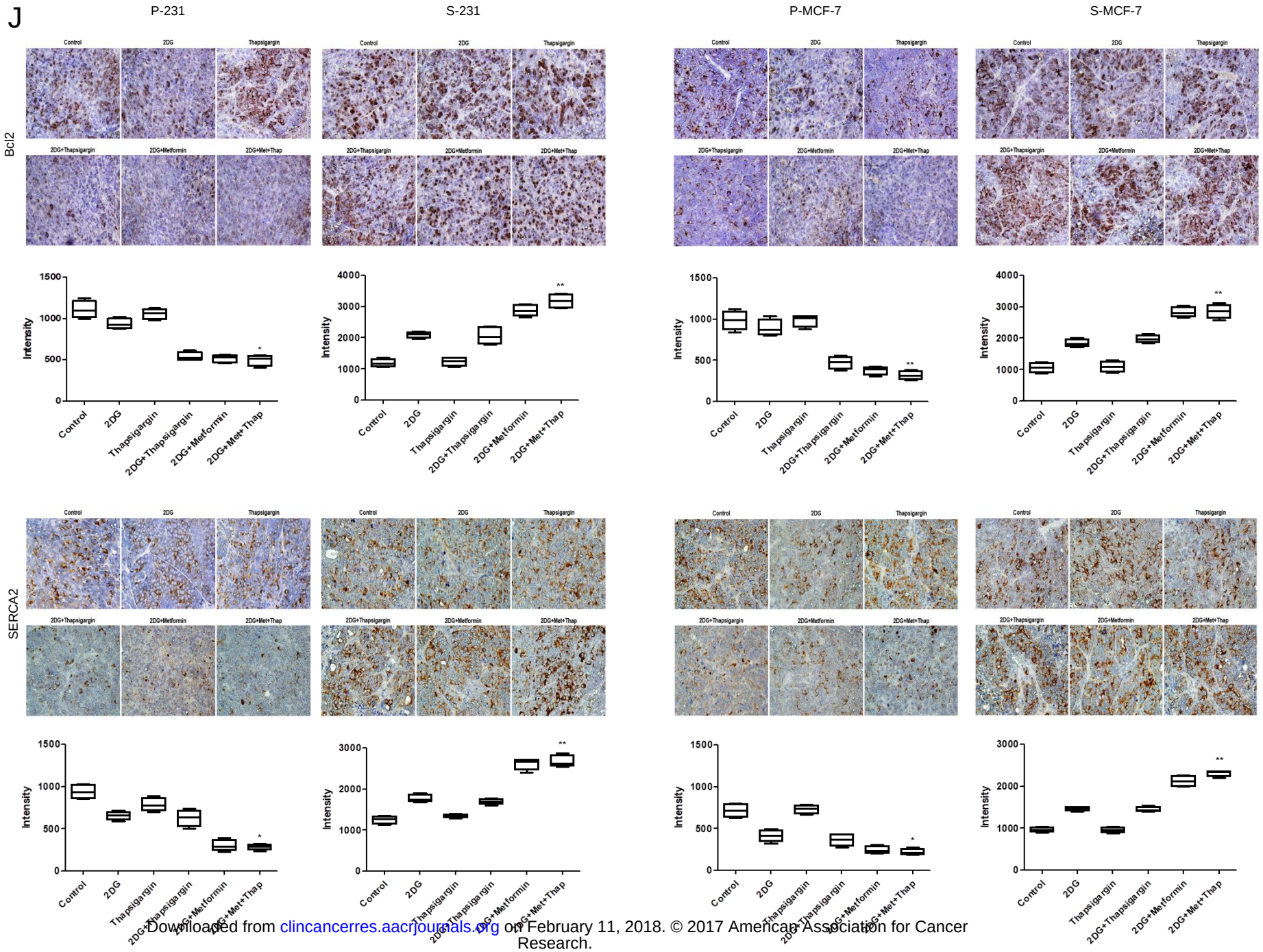

AACR American Association for Cancer Research

Clinical Cancer Research

Survival of cancer stem-like cells under metabolic stress via CaMK2 α-mediated upregulation of sarco/endoplasmic reticulum calcium ATPase expression

Ki Cheong Park, Seung Won Kim, Jeong Yong Jeon, et al.

Clin Cancer Res Published OnlineFirst December 26, 2017.